

000 001 002 003 004 005 006 007 008 009 010 FROM BIAS TO BENEFIT: PLACE GOOD DOCUMENTS IN GOOD POSITIONS

011
012
013
014
015
016
017
018
019
020
021
022
023
024
Anonymous authors
025
026
027
028
029
030
031
032
033
034
035
036
037
038
039
040
041
042
043
044
045
046
047
048
049
050
051
052
053

Paper under double-blind review

ABSTRACT

Large language models (LLMs) exhibit a U-shaped positional bias in processing input information, characterized by heightened attention to tokens at the beginning and end of the prompt while ignoring information in the middle, also known as the Lost-in-the-Middle phenomenon. In this paper, we investigate the internal mechanisms underlying this phenomenon by analyzing how positional bias influences attention weights across both horizontal (input-level) and vertical (layer-level) dimensions of the model. Based on these findings, we propose U-shaped Placement, a strategy that leverages inherent positional bias of the model by assigning documents to positions that align with its attention pattern. By combining this placement strategy with the importance estimations of documents, effectively placing good documents in good positions, we enhance the model’s ability to utilize documents within two iterations. Experimental results demonstrate that our method consistently outperforms existing baselines across multiple models and datasets, indicating that leveraging positional bias can bring improved document utilization capability. Our codes are submitted with the paper and will be publicly available.

1 INTRODUCTION

As large language models(LLM) continue to evolve, they have achieved superior performance in many tasks, especially in Question Answering (QA) tasks (Touvron et al., 2023; Achiam et al., 2023; DeepSeek-AI, 2025). Furthermore, Retrieval Augmented Generation(RAG) has become a widely recognized paradigm by supplementing the model with external knowledge in the form of context, which helps to improve the factual accuracy and reliability of the answers (Gao et al., 2023; Asai et al., 2023). However, the quality of input documents is variable (Shi et al., 2023; Yoran et al., 2024; Wu et al., 2024) due to the inadequate performance of the retriever (Yan et al., 2024) or the alignment gap between the retriever and the generator (Ke et al., 2024; Li & Ramakrishnan, 2025).

How to improve a model’s ability to utilize documents with inputs of varying quality is a challenging and realistic research topic, and this is also part of the model robustness problem (Shi et al., 2023; Yoran et al., 2024; Zhou et al., 2025). Previous works improve the robustness of the model by incorporating irrelevant and interfering documents into the supervised fine-tuning process (Pan et al., 2024; Yoran et al., 2024; Tu et al., 2025), which is customized and requires additional training resources. Instead of direct training, we focus on the model’s properties of prompt utilization, especially the ability to leverage documents in different positions.

The retrieval results convey the relative importance of documents through their ranking and order in the prompt (Gao et al., 2023). But language models exhibit a U-shaped positional bias in processing input information, assigning greater weight to content at the beginning and end of the prompt while often ignoring content in the middle. This phenomenon was initially identified in Liu et al. (2024) and later corroborated through performance evaluations in RAG tasks by Cuconasu et al. (2024) and Wu et al. (2024). However, research on the underlying mechanisms of this U-shaped curve, as revealed through the model’s internal states, remains limited.

In this paper, we first analyze the positional bias towards documents by examining the internal mechanisms of LLMs. We assess the influence of document position on attention weights from both horizontal (input-level) and vertical (layer-level) perspectives, using systematically constructed inputs and probing different layers of the model. The value of attention weight not only captures document relevance but also encapsulates the influence of positional bias (Peysakhovich & Lerer,

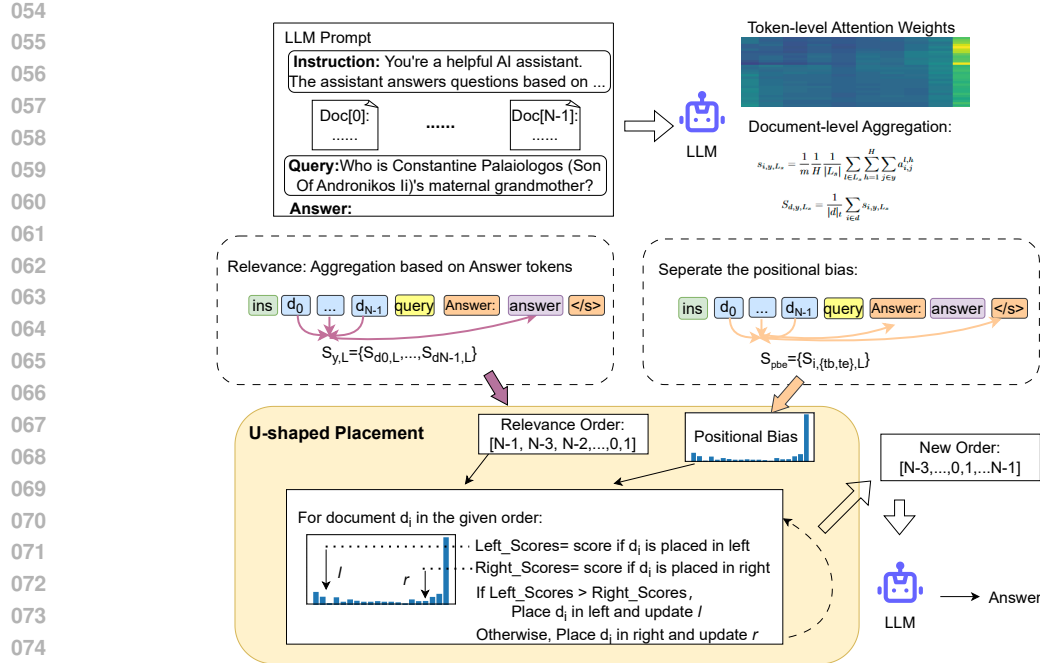


Figure 1: The framework of our proposed pipeline.

2023; Chen et al., 2024; Liu et al., 2025). Our analysis isolates the positional effect and confirms that it consistently follows the U-shaped curve.

Building upon these insights, we propose U-shaped Placement, a strategy that reorganizes documents to align with the model’s inherent positional bias. This approach is integrated into a two-round iterative generation process that refines input prompts based on the model’s internal states, as depicted in Figure 1. Specifically, during the first round, we compute document importance scores using attention weights and simultaneously estimate the model’s positional bias. These two signals are then combined to rearrange documents for the second iteration, ensuring that content deemed most relevant is placed in positions that receive higher attention. We conduct comprehensive experiments on several multi-document QA datasets utilizing various commonly used LLMs, demonstrating that our method consistently outperforms baselines and yields higher response quality, indicating that leveraging positional bias can bring improved document utilization capability. Our method requires no additional training and can be readily applied to different models and datasets.

Our contributions are as follows: (1) We study the influence of document position on attention weights from both horizontal (input-level) and vertical (layer-level) perspectives, revealing the internal mechanisms underlying the Lost-in-the-Middle phenomenon. (2) We propose a novel strategy called U-shaped Placement to take advantage of inherent positional bias in the generation process, which is the first to our knowledge. (3) Comprehensive experiments show that our method can improve the effectiveness of document utilization in a training-free manner.

2 RELATED WORKS

2.1 RETRIEVAL AUGMENTED GENERATION

Retrieval-augmented generation (RAG) has exhibited significant effectiveness in addressing issues such as hallucinations by introducing external knowledge into context or training objectives (Gao et al., 2023; Asai et al., 2023; Tu et al., 2025; Luo et al., 2024; 2025). However, irrelevant and distracting information can adversely affect the generated results (Shi et al., 2023; Yoran et al., 2024; Wu et al., 2024). Previous work has explored various improvement strategies, such as improving the retriever (Shi et al., 2024), designing new rerankers (Kim & Lee, 2024), investigating gaps between

108 the retriever and generator (Ke et al., 2024; Li & Ramakrishnan, 2025), and improving the robustness
 109 of the LLM, especially interference resistance (Xiang et al., 2024; Yoran et al., 2024). Rather than
 110 directly adding documents to the training or supervised fine-tuning process (Pan et al., 2024; Yoran
 111 et al., 2024; Tu et al., 2025), we study the internal utilization characteristic of documents at different
 112 positions and dynamically modify inputs based on positional bias to improve robustness.
 113

114 2.2 DOCUMENT RELEVANCE

116 In RAG pipeline, the external retriever or reranker will give a relevance score, and the different
 117 importance would be reflected mainly by the positional order in prompt, rather than the value it-
 118 self (Gao et al., 2023; Shi et al., 2024; Kim & Lee, 2024). Including the relevance score into the
 119 prompts may affect the generated results (Pan et al., 2024), but this requires a high level of the
 120 instruction-following ability. In addition to utilizing externally given relevance scores, there are also
 121 some works that let the model itself give a judgment on the relevance of documents through prompt
 122 engineering (Qin et al., 2024; Sun et al., 2023; Niu et al., 2024), adding probing structures (Baek
 123 et al., 2024; Wang et al., 2024), or internal attention weight (Peysakhovich & Lerer, 2023; Chen
 124 et al., 2024; Liu et al., 2025). We also use attention weights as the basis for model importance esti-
 125 mation for documents, but we compute them differently and further combine them with positional
 126 bias to optimize the inputs.
 127

128 2.3 POSITIONAL BIAS

129 The LLMs are unable to treat the information in the prompt equally and have a positional bias, which
 130 is part of the model’s prompt-sensitive properties (Xie et al., 2024). It tends to pay more attention to
 131 information at the beginning and the end, and to ignore those in the middle, which is characterized by
 132 a U-shape curve. This “Lost in the Middle” phenomenon was first identified in Liu et al. (2024). To
 133 date, many RAG and long text-related works (Cuconasu et al., 2024; Wu et al., 2024; Xu et al., 2024)
 134 have investigated this issue by showing the performance difference caused by positional bias. We
 135 study this phenomenon from internal attention weight of the LLM both horizontally and vertically,
 136 offering a new perspective to investigate the U-shaped positional bias, and we propose a method to
 137 take advantage of positional bias during the generation process.
 138

139 3 INVESTIGATION ON POSITIONAL BIAS

140 In this section, we investigate the model’s positional bias and relevance assessment toward docu-
 141 ments placed at different prompt locations. Building upon empirical performance variations ob-
 142 served across positions, we further analyze these behaviors through the model’s internal states, with
 143 a particular focus on attention weights.
 144

145 3.1 NOTATIONS

146 We formulate the task as generating the answer based on a given question and retrieved documents,
 147 following standard RAG settings. For each sample, we use q to present the question. The retrieval
 148 documents are denoted as $D = \{d_0, d_1, \dots, d_{N-1}\}$, where d_i is a single document, and N is the total
 149 number of documents. $x = \{x_0, x_1, \dots, x_{k-1}\}$ is the input of large language models, where k is the
 150 number of tokens contained in the input, i.e., the token length. The input x is constructed based on q ,
 151 D , and a certain prompt template T . And the output answer is indicated as $y = \{y_0, y_1, \dots, y_{m-1}\}$,
 152 where m is the token length of y . The language model is presented as θ and generates each token in
 153 y with auto-regressive style.
 154

155 3.2 PRELIMINARY EXPERIMENTS

156 To demonstrate the effect of position, we first compare model performance under two standard
 157 configurations: unordered documents and documents ordered by external relevance. These settings
 158 represent common practices in both RAG evaluations and practical scenarios.
 159

160 **Datasets** We apply the datasets processed by Pan et al. (2024), which include both random-
 161 ized (denoted as *Unordered*) and relevance-ordered (denoted as *Ordered*) versions to minimize

162 processing-related randomness. Due to computational constraints, our experiments are conducted
 163 on three widely-used open-domain multi-document QA benchmarks: HotpotQA (Yang et al., 2018),
 164 Musique (Trivedi et al., 2022), and 2WikiMHQA (Ho et al., 2020). The details of datasets can be
 165 found in the original paper or Appendix B.1.
 166

167 **Models and Metrics** We test four popular open-source LLMs: Vicuna-7B (Chiang et al., 2023),
 168 Llama-3.1-8B (Dubey et al., 2024), Qwen2.5-7B and Qwen2.5-7B-Instruct (Yang et al., 2024). We
 169 follow Pan et al. (2024) and utilize Exact Match (EM) as the primary evaluation metric, which
 170 checks whether the short answers provided are exact substrings of the generation.
 171

172 **Implementation** Hyperparameters including temperature and instruction format remain consistent
 173 with their setup. Unlike their work, however, we conduct experiments under a zero-shot setting
 174 to better isolate and examine the model’s intrinsic positional bias and relevance assessment mecha-
 175 nisms. The placement of documents in the prompt adheres to Pan et al. (2024), positioning the most
 176 relevant documents closest to the question when documents are ordered. Previous researches (Cu-
 177 conasu et al., 2024; Liu et al., 2025) have also confirmed that this placement is a widely applied
 178 paradigm and strong baseline. Additional details regarding prompt templates and implementation
 179 are provided in Appendix B.2.
 180

181 Table 1: Original zero-shot model performance in HotpotQA(H), Musique(M) and
 182 2WikiMHQA(W) datasets of CAGB benchmark (Pan et al., 2024).

Prompt	Vicuna-7b			Llama-3.1-8b			Qwen2.5-7b			Qwen2.5-7b-ins		
	H	M	W	H	M	W	H	M	W	H	M	W
Unordered	0.392	0.238	0.452	0.292	0.192	0.35	0.376	0.298	0.39	0.468	0.458	0.48
Ordered	0.4	0.312	0.482	0.302	0.238	0.358	0.408	0.342	0.41	0.472	0.5	0.526

183 The results of the EM values are presented in Table 1. The observed inconsistency with the results
 184 reported in Pan et al. (2024) can be primarily attributed to our use of a zero-shot evaluation setting,
 185 along with potential discrepancies in huggingface versions and hardware configurations. The re-
 186 sults indicate that, although performance varies across models and datasets, all models are affected
 187 by document position and unable to utilize information from each position equally, confirming the
 188 prevalence of positional bias. As the number of documents increases, the effect of position be-
 189 comes more pronounced. This is clearly demonstrated by the Musique dataset, which contains 20
 190 documents and exhibits substantially greater sensitivity to ordering changes.
 191

192 To conduct a more fine-grained study of the varying effects at different positions, we explore the
 193 dependency of the generated answer token on the context documents using the metric developed by
 194 Qi et al. (2024), called MIRAGE. Since this metric also analyzes the generated results and is not the
 195 focus of this paper, we provide the corresponding experimental details and results in the Appendix
 196 C. These results similarly indicate the existence of positional bias, showing that the model relies
 197 more on documents placed at the beginning and end of the input.
 198

202 3.3 ATTENTION WEIGHT

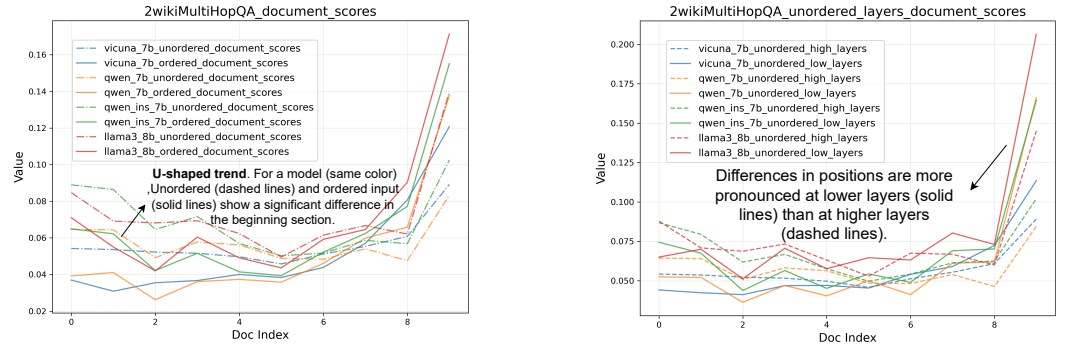
203 Both downstream performance and the MIRAGE metric reflect the presence of positional bias. In
 204 this section, we investigate the underlying mechanisms and internal states of the model. Attention
 205 weights capture, at the token level, the influence of context tokens on answer tokens during genera-
 206 tion. To assess this influence at the document level, we aggregate attention weights as follows:
 207

$$s_{i,y,L_s} = \frac{1}{m} \frac{1}{H} \frac{1}{|L_s|} \sum_{l \in L_s} \sum_{h=1}^H \sum_{j \in y} a_{i,j}^{l,h} \quad (1)$$

$$S_{d,y,L_s} = \frac{1}{|d|_t} \sum_{i \in d} s_{i,y,L_s} \quad (2)$$

208 where $a_{i,j}^{l,h}$ denotes the attention weight from the token i (from the document d whose token length
 209 is $|d|_t$) to the token j (from the answer y whose token length is m) by the attention head h at layer
 210

l, *H* is the total number of attention heads, and L_s is the set of selected layers. After obtaining the influence score of each token in the document on the answer at token level (s_{i,y,L_s}), we then aggregate and normalize by removing the influence of length to obtain attention weight value at document level for the answer (S_{d,y,L_s}). $S_{y,L_s} = \{S_{d_0,y,L_s}, \dots, S_{d_{N-1},y,L_s}\}$ is the overall set of document scores.



(a) Horizontal analysis: document scores $S_{y,L_{all}}$ under unordered and ordered input.
(b) Vertical analysis: document scores S_{y,L_s} with different selected layers under unordered input.

Figure 2: The document scores of all models on 2wikiMultiHopQA datasets. The results of the same model are shown in the same color.

We then analyze the effect of position on document-level scores from both horizontal and vertical perspectives. Horizontally, we compare document scores across different positions under varying input conditions. We first set L_s to all layers and calculate $S_{y,L_{all}}$. To ensure robustness, we randomly sample 50 instances from the 2WikiMultiHopQA dataset and average the results for clearer visualization, as shown in Figure 2a. Complete results across all models and datasets are provided in Appendix D.1. The results indicate that document scores $S_{y,L_{all}}$ exhibit a U-shaped distribution across positions under both ordered and unordered input conditions. However, under ordered input, the U-shaped curve is more skewed toward the end of the input (closer to the question), displaying a steeper profile. In contrast, the U-shape under unordered input is gentler, with less pronounced disparities between the beginning and the end portion. These findings suggest that the model’s internal estimation of document importance is influenced by positional bias in a U-shaped manner, and the extent of this bias varies with the ordering of input documents.

From a vertical perspective, we further examine the effect of different layer selections under the same prompt. We partition all layers into lower and higher halves and compare the document scores derived from each group. To clearly illustrate the U-shaped positional bias with minimal interference from document relevance, we present results using unordered inputs on the 2WikiMultihopQA dataset in Figure 2b, as unordered inputs make positional bias more evident and standard than ordered inputs. Complete results are available in Appendix D.2. The results indicate that although the absolute values of document scores differ between the lower and higher layers, both exhibit a similar U-shaped trend across positions. Notably, positional distinctions are more pronounced in the lower layers. This observation aligns with the widely accepted view that lower layers are more sensitive to positional information, while higher layers focus on processing semantic content.

4 SEPARATE AND UTILIZE POSITIONAL BIAS

The attention weight reflects the overall influence of context tokens on answer tokens, including semantic relevance and positional influence. How to directly obtain the positional influence in the generation process is a problem worth studying.

While prior work has employed meaningless queries to study attention patterns (Chen et al., 2024), this approach necessitates an additional LLM call and focuses on query tokens rather than answer tokens. In our method, we aggregate attention weights corresponding to the token immediately preceding the answer and the terminating token (highlighted in orange in Figure 1). This choice is motivated by the observation that the token preceding the answer (e.g., “is” or “:”) typically

270 carries little semantic information. By integrating attention scores from both the beginning and the
 271 end of the answer, we construct a composite representation of the overall positional characteristics
 272 associated with the answer tokens. This strategy aligns with the intuitive notion that combining start
 273 and end positional cues can effectively approximate the holistic positional information.

274 As lower layers have been shown to capture
 275 positional signals more explicitly, we perform
 276 this aggregation over a selected set of lower
 277 layers, denoted as L_l . We visualize the re-
 278 sulting scores $S_{\{t_b, t_e\}, L_l}$ for the 2WikiMulti-
 279 hopQA dataset in Figure 3. Results for other
 280 datasets are provided in Appendix D.3. In con-
 281 trast to the document-level scores shown in Fig-
 282 ure 2a, these positional scores exhibit no signif-
 283 icant variation between unordered and ordered
 284 inputs. This suggests that our aggregated re-
 285 presentation effectively captures general positional
 286 characteristics of the answer, largely indepen-
 287 dent of document ordering.

288 After separating the positional bias, we hope to
 289 use it to improve the model’s ability to utilize documents. A straightforward strategy would be to
 290 rank documents directly according to the aggregated score $S_{\{t_b, t_e\}, L_l}$, from most to least preferred.
 291 However, this approach encounters a practical issue related to length variability. Since $S_{\{t_b, t_e\}, L_l}$ is
 292 length-normalized, the actual token capacity associated with each score may vary significantly. For
 293 example, the position with the highest score may only contain 100 token positions, and placing a
 294 document with more than 100 tokens will use the positions corresponding to other scores. To address
 295 this issue, we operate directly on token-level scores $s_{i, \{t_b, t_e\}, L_l}$ rather than document-level aggre-
 296 gates. The underlying intuition remains consistent: to place high-quality documents in positions that
 297 receive higher attention. Concretely, we propose an allocation algorithm that considers documents
 298 in descending order of relevance and uses the U-shaped attention profile to place each document to
 299 either the beginning or the end of the available prompt space. At each step, the algorithm evaluates
 300 whether placing the document on the left (beginning) or right (end) of the remaining context yields
 301 a higher token-level score, and assigns it accordingly. This process continues until all documents
 302 are placed, resulting in a U-shaped arrangement that aligns with the model’s inherent attention bias.
 303 The complete procedure, termed U-shaped Placement, is formalized in pseudocode in Algorithm 1.

Algorithm 1 U-shaped Placement

Input Relevance ranking R , attention weight A_θ , preceding token t_b and terminating token t_e of
 306 answer, the collection of token lengths for all documents $T_l = \{T_0, \dots, T_{N-1} | T_i = |d_i|_t\}$.
 307 1: Ensure that the relevant ones in R come first;
 308 2: Get $S_{pbe} = \{s_{i, \{t_b, t_e\}, L_l}\}$ based on A_θ ; \triangleright equation 1
 309 3: Initialization: $l = 0, r = \sum_{i=0}^{N-1} T_i, l_{idx} = 0, r_{idx} = N - 1, R_u = [0] * N$;
 310 4: **for** $i \in R$ **do**
 311 5: $T_i = T_l[i]$;
 312 6: Left_Scores = $S_{pbe}[l : l + T_i].sum()$;
 313 7: Right_Scores = $S_{pbe}[r - T_i : r].sum()$;
 314 8: **if** Right_Scores \geq Left_Scores **then**
 315 9: $R_u[r_{idx}] = i, r_{idx} = r_{idx} - 1, r = r - T_i$;
 316 10: **else**
 317 11: $R_u[l_{idx}] = i, l_{idx} = l_{idx} + 1, l = l + T_i$;
 318 12: **end if**
 319 13: **end for**
 320 **Output:** The new ranking R_u

321
 322 The U-shaped Placement approach can be combined with all kinds of document ranking methods.
 323 We combine it with the previously obtained document scores that are aggregated based on the answer
 tokens, and modify the inputs for the next round, thus improving the overall ability of the model to

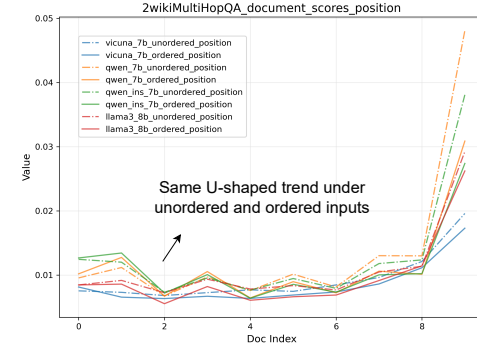


Figure 3: The positional scores $S_{\{t_b, t_e\}, L_l}$ on 2wikiMultiHopQA datasets.

324 utilize documents. The complete pipeline is summarized in pseudocode in Algorithm 2, where L_l
 325 and L_h denote the lower and higher halves of the model layers, respectively.
 326

327 Algorithm 2 Place Good Documents in Good Positions

329 **Input** Prompt Template T , LLM θ , Question q , Documents $D = \{d_0, \dots, d_{N-1}\}$.
 330 1: Construct input: $x = T(q, D)$;
 331 2: Get the output from LLM: $y, A_\theta = \theta(x)$;
 332 3: Calculate S_{y, L_h} ; \triangleright equation 2
 333 4: Rank the documents based on S_{y, L_h} as R_a ;
 334 5: Get token lengths of each document from x to construct T_l , and locate t_b and t_e from x ;
 335 6: $R_u = \text{U-shaped Placement}(R_a, A_\theta, t_b, t_e, T_l)$;
 336 7: Reconstruct the input based on R_u : $x_u = T(q, R_u(D))$;
 337 8: Get the final answer: $y = \theta(x_u)$
Output: The output answer y

339
 340 The algorithm is essentially two rounds of iterations of the LLM, using the attention weight from the
 341 first round to obtain the model’s ranking of the documents and positional bias, and then placing good
 342 documents in good positions according to the U-shape, and reconstructing the inputs to generate the
 343 final answer in the second round.

344
345 5 EXPERIMENTS

346
347 5.1 BASELINES

348 The basic setting of the experiment is the same as preliminary experiments in section 3.2, including
 349 the datasets, models, metrics, and so on.

351 Our work is essentially a two-round iteration of the LLM, so we mainly consider similarly set-
 352 up baselines for fair comparison, and the following is a brief description of the baselines we
 353 consider: **(1)Vanilla**: The most basic baseline, generating answers directly based on inputs.
 354 **(2)RankGPT** (Sun et al., 2023): Two rounds of iteration, the first round uses the model to sort
 355 the documents in listwise style and the second round generates the answer. The prompt template
 356 used in the first round is shown in the Appendix F. **(3)Attention Sorting** (Peysakhovich & Lerer,
 357 2023): Two rounds of iteration, average per-document attention is computed for the first generated
 358 token in the first round, and then documents are sorted based on the attention scores for the second
 359 round. **(4)ICR** (Chen et al., 2024): Two rounds of iteration, the first round aggregates the contextual
 360 attention weight corresponding to all query tokens and calibrates it with the meaningless query to
 361 get the document order, and the second round generates the answers based on the reordered docu-
 362 ment. **(5)SELFELICIT** (Liu et al., 2025): Two rounds of iteration, average per-sentence attention
 363 is computed for the first generated token in the first round and then important sentences are selected
 364 to be emphasized with special token in the input for the second round.

365
366 5.2 MAIN RESULTS

367 The results are shown in Table 2. The results show that: (1) Our method outperforms previous
 368 baselines on most datasets and models, under both unordered and ordered input settings. (2) Im-
 369 provements are more substantial under unordered inputs than under ordered inputs. This can be
 370 partly attributed to the greater potential for enhancement in unordered settings. Notably, our
 371 approach applied to unordered inputs can surpass the performance of the vanilla ordered baseline that
 372 relies on external retrieval rankings, demonstrating its ability to infer an effective document order
 373 even without prior ranking. The gains under ordered inputs further confirm that our method enhances
 374 the model’s capacity to utilize documents effectively. (3) Improvements are more pronounced on
 375 datasets with more documents, such as Musique. And our method can be applied to experiments
 376 involving any number of documents, which is proved in section 6.3. In terms of models, greater
 377 gains are observed on the Qwen series compared to Vicuna-7b, which may be related to the base
 378 capability of the model: stronger models provide more reliable internal state signals. Nevertheless,
 379 our method delivers consistent performance improvements across diverse models and datasets.

378 Table 2: Zero-shot model performance in HotpotQA(H), Musique(M) and 2WikiMHQA(W)
 379 datasets of CAGB benchmark (Pan et al., 2024). See section 5.1 for more details on baselines.
 380

381 Prompt	382 Methods	383 Vicuna-7b			384 Llama-3.1-8b			385 Qwen2.5-7b			386 Qwen2.5-7b-ins		
		387 H	388 M	389 W	390 H	391 M	392 W	393 H	394 M	395 W	396 H	397 M	398 W
399 Unordered	Vanilla	0.392	0.238	0.452	0.292	0.192	0.35	0.376	0.298	0.39	0.468	0.458	0.48
	RankGPT	0.401	0.22	0.46	0.278	0.196	0.334	0.372	0.343	0.402	0.466	0.51	0.526
	AttentionSort	0.386	0.291	0.484	0.296	0.216	0.336	0.398	0.375	0.4	0.462	0.495	0.484
	ICR	0.421	0.305	0.498	0.298	0.237	0.368	0.379	0.385	0.384	0.469	0.511	0.522
	SELFELICIT	0.378	0.257	0.462	0.308	0.229	0.359	0.393	0.298	0.43	0.417	0.311	0.382
	Our	0.414	0.31	0.506	0.302	0.245	0.372	0.402	0.393	0.434	0.482	0.513	0.536
400 Ordered	Vanilla	0.4	0.312	0.482	0.302	0.238	0.358	0.408	0.342	0.41	0.472	0.5	0.526
	RankGPT	0.403	0.28	0.502	0.284	0.21	0.342	0.391	0.358	0.416	0.493	0.516	0.53
	AttentionSort	0.404	0.3	0.474	0.294	0.218	0.342	0.408	0.385	0.432	0.492	0.485	0.518
	ICR	0.413	0.307	0.512	0.301	0.254	0.353	0.406	0.378	0.4	0.487	0.537	0.504
	SELFELICIT	0.393	0.314	0.482	0.314	0.261	0.372	0.411	0.342	0.432	0.417	0.447	0.372
	Our	0.426	0.315	0.51	0.304	0.267	0.378	0.412	0.401	0.436	0.495	0.555	0.542

393 6 ANALYSIS

394 The pipeline comprises two key components: deriving document order and positional bias from the
 395 model’s internal states. While the combined effect of these components has been validated in the
 396 main experiments, this section examines their individual contributions. Some additional attempts
 397 are presented in Appendix G.

400 6.1 THE INFLUENCE OF POSITIONS

401 We introduce the U-shaped Placement strategy to organize document positions in accordance with
 402 the model’s positional bias. This method is compatible with any document relevance ordering,
 403 regardless of the ranking method employed. In this section, we utilize an external relevance ranking
 404 and focus on assessing the effect of document placement.

405 We evaluate four placement strategies: placing relevant documents near the question, U-shaped
 406 Placement, and the reverse variants of both. In the original versions, higher-relevance documents are
 407 assigned to positions that inherently receive more attention, while the reverse versions deliberately
 408 assign lower-relevance documents to these favored positions. All four configurations use identical
 409 prompt templates, varying only in document order, thereby isolating the effect of placement on
 410 model performance. We’ve included an example in the Appendix E for better explanation.

411 Table 3: Results of different placements with relevance ranking based on external retrieval. Default
 412 means placing the relevant ones close to question, while U-shaped is our method in accordance with
 413 positional bias. Different settings indicate whether a good position is preferentially occupied by a
 414 good (original) or bad (reverse) document.

417 Placement	418 Setting	419 Vicuna-7b			420 Llama-3.1-8b			421 Qwen2.5-7b			422 Qwen2.5-7b-ins		
		423 H	424 M	425 W	426 H	427 M	428 W	429 H	430 M	431 W	432 H	433 M	434 W
435 Default	Original	0.4	0.312	0.482	0.302	0.238	0.358	0.408	0.342	0.41	0.472	0.5	0.526
	Reverse	0.378	0.24	0.464	0.28	0.2	0.348	0.37	0.323	0.39	0.456	0.477	0.5
436 U-shaped (Our)	Original	0.397	0.314	0.524	0.31	0.252	0.376	0.416	0.369	0.414	0.486	0.509	0.522
	Reverse	0.367	0.216	0.446	0.268	0.186	0.338	0.368	0.3	0.39	0.454	0.435	0.476

437 The results in Table 3 demonstrate that: (1) The proposed U-shaped Placement, which aligns with
 438 the model’s positional bias, represents a more effective placement strategy that enhances the model’s
 439 ability to utilize documents. When compared with the results in Table 2, the performance of Vicuna-
 440 7b and Llama-3.1-8b models approaches or even exceeds that in the main experiments, whereas
 441 the Qwen series still lags behind. This observation aligns with earlier findings regarding model
 442 capabilities, suggesting that relevance rankings produced by the Qwen series are comparatively
 443 more reliable. (2) Among the reverse placement configurations, the reversed U-shaped Placement
 444 leads to the most significant performance degradation, underscoring the importance of leveraging
 445 positional bias.

432 6.2 DOCUMENT RELEVANCE
433434 In prior analyses, we aggregated attention weights from context tokens to answer tokens to estimate
435 document importance. In this section, we investigate the effect of different document relevance sorting
436 methods and aggregation strategies, mainly considering aggregation based on the first generated
437 token or query tokens involved in the previous works.438 Table 4: Results of the different document relevance sorting methods of vicuna-7b model.
439

Level	Source	H	M	W
Document-Level	Retrieval	0.4	0.312	0.482
	RankGPT	0.403	0.28	0.502
Token-level	First Token	0.404	0.291	0.48
	Query	0.398	0.301	0.49
	Answer	0.406	0.305	0.494
	Answer(qwen)	0.412	0.329	0.512

448 To exclude positional effect, we adopt the default ranking strategy, which places the most relevant
449 documents closest to the question. Results of vicuna-7b in Table 4 show that: (1) Aggregation based
450 on answer tokens outperforms document-level, query-based and first-token-based approaches, as
451 it more directly captures influence on the generated answer. (2) As mentioned before, document
452 relevance rankings derived from Qwen models are more reliable. Providing such rankings to Vicuna
453 improves its performance, suggesting a promising direction for hybrid approaches that leverage
454 multiple models during generation.455 6.3 THE NUMBER OF DOCUMENTS
456457 While the main experiments validate the effectiveness of our method on datasets containing 10 and
458 20 documents, we also conducted additional experiments with fewer input documents to assess its
459 versatility and efficacy. We take the original ten-document 2wikiMultiHopQA dataset and only
460 intercepted the first three and five documents for the experiment. Experimental results in the Table
461 5 demonstrate that our proposed ranking method and U-shaped Placement remain high efficiency
462 across varying numbers of documents.463 Table 5: Results of varying number of input documents.
464

Prompt	Methods	Vicuna-7b			Qwen2.5-7b-ins		
		3doc	5doc	10doc	3doc	5doc	10doc
Unordered	Vanilla + Default	0.286	0.296	0.452	0.316	0.334	0.48
	Vanilla + U-shaped	0.334	0.35	0.48	0.34	0.358	0.501
	Our Ranking + Default	0.344	0.358	0.474	0.342	0.35	0.51
	Our Ranking + U-shaped	0.356	0.374	0.506	0.35	0.36	0.536
Ordered	Vanilla + Default	0.38	0.424	0.482	0.366	0.428	0.526
	Vanilla + U-shaped	0.398	0.47	0.524	0.37	0.464	0.522
	Our Ranking + Default	0.39	0.456	0.494	0.376	0.444	0.53
	Our Ranking + U-shaped	0.401	0.463	0.51	0.394	0.466	0.542

475 7 CONCLUSION
476477 In this paper, we investigate the positional bias based on model’s attention weight, both horizontally
478 and vertically. We find that the model’s estimation of document importance is also internally affected
479 by positional bias in a U-shape, with the magnitude of the U-shape varying with the order of input
480 documents. In addition, the lower layers reflect the position information more significantly.
481482 And we propose U-shaped Placement to separate and utilize positional bias. Combining it with the
483 importance estimation of documents within the model, placing good documents in good positions,
484 can improve the model’s ability to utilize documents within two iterations. Our approach requires
485 no training, and can work on any open-source model and dataset.

486 REFERENCES
487

488 OpenAI Josh Achiam, Steven Adler, Sandhini Agarwal, Lama Ahmad, Ilge Akkaya, Florencia Leoni
489 Aleman, Diogo Almeida, Janko Altenschmidt, Sam Altman, Shyamal Anadkat, Red Avila, Igor
490 Babuschkin, Suchir Balaji, Valerie Balcom, Paul Baltescu, Haiming Bao, Mo Bavarian, Jeff Bel-
491 gum, Irwan Bello, Jake Berdine, Gabriel Bernadett-Shapiro, Christopher Berner, Lenny Bog-
492 donoff, Oleg Boiko, Madelaine Boyd, Anna-Luisa Brakman, Greg Brockman, Tim Brooks, Miles
493 Brundage, Kevin Button, Trevor Cai, Rosie Campbell, Andrew Cann, Brittany Carey, Chelsea
494 Carlson, Rory Carmichael, Brooke Chan, Che Chang, Fotis Chantzis, Derek Chen, Sully Chen,
495 Ruby Chen, Jason Chen, Mark Chen, Benjamin Chess, Chester Cho, Casey Chu, Hyung Won
496 Chung, Dave Cummings, Jeremiah Currier, Yunxing Dai, Cory Decareaux, Thomas Degry, Noah
497 Deutsch, Damien Deville, Arka Dhar, David Dohan, Steve Dowling, Sheila Dunning, Adrien
498 Ecoffet, Atty Eleti, Tyna Eloundou, David Farhi, Liam Fedus, Niko Felix, Sim'on Posada Fish-
499 man, Juston Forte, Isabella Fulford, Leo Gao, Elie Georges, Christian Gibson, Vik Goel, Tarun
500 Gogineni, Gabriel Goh, Raphael Gontijo-Lopes, Jonathan Gordon, Morgan Grafstein, Scott Gray,
501 Ryan Greene, Joshua Gross, Shixiang Shane Gu, Yufei Guo, Chris Hallacy, Jesse Han, Jeff Har-
502 rris, Yuchen He, Mike Heaton, Johannes Heidecke, Chris Hesse, Alan Hickey, Wade Hickey, Peter
503 Hoeschele, Brandon Houghton, Kenny Hsu, Shengli Hu, Xin Hu, Joost Huizinga, Shantanu Jain,
504 Shawn Jain, Joanne Jang, Angela Jiang, Roger Jiang, Haozhun Jin, Denny Jin, Shino Jomoto,
505 Billie Jonn, Heewoo Jun, Tomer Kaftan, Lukasz Kaiser, Ali Kamali, Ingmar Kanitscheider, Ni-
506 tish Shirish Keskar, Tabarak Khan, Logan Kilpatrick, Jong Wook Kim, Christina Kim, Yongjik
507 Kim, Hendrik Kirchner, Jamie Ryan Kiros, Matthew Knight, Daniel Kokotajlo, Lukasz Kon-
508 draciuk, Andrew Kondrich, Aris Konstantinidis, Kyle Koscic, Gretchen Krueger, Vishal Kuo,
509 Michael Lampe, Ikai Lan, Teddy Lee, Jan Leike, Jade Leung, Daniel Levy, Chak Ming Li,
510 Rachel Lim, Molly Lin, Stephanie Lin, Mateusz Litwin, Theresa Lopez, Ryan Lowe, Patricia
511 Lue, Anna Adeola Makanju, Kim Malfacini, Sam Manning, Todor Markov, Yaniv Markovski,
512 Bianca Martin, Katie Mayer, Andrew Mayne, Bob McGrew, Scott Mayer McKinney, Christine
513 McLeavey, Paul McMillan, Jake McNeil, David Medina, Aalok Mehta, Jacob Menick, Luke
514 Metz, Andrey Mishchenko, Pamela Mishkin, Vinnie Monaco, Evan Morikawa, Daniel P. Mossing,
515 Tong Mu, Mira Murati, Oleg Murk, David M'ely, Ashvin Nair, Reiichiro Nakano, Rajeev Nayak,
516 Arvind Neelakantan, Richard Ngo, Hyeonwoo Noh, Ouyang Long, Cullen O'Keefe, Jakub W.
517 Pachocki, Alex Paino, Joe Palermo, Ashley Pantuliano, Giambattista Parascandolo, Joel Parish,
518 Emy Parparita, Alexandre Passos, Mikhail Pavlov, Andrew Peng, Adam Perelman, Filipe de Avila
519 Belbute Peres, Michael Petrov, Henrique Pondé de Oliveira Pinto, Michael Pokorny, Michelle
520 Pokrass, Vitchyr H. Pong, Tolly Powell, Alethea Power, Boris Power, Elizabeth Proehl, Raul
521 Puri, Alec Radford, Jack Rae, Aditya Ramesh, Cameron Raymond, Francis Real, Kendra Rim-
522 bach, Carl Ross, Bob Rotsted, Henri Roussez, Nick Ryder, Mario D. Saltarelli, Ted Sanders,
523 Shibani Santurkar, Girish Sastry, Heather Schmidt, David Schnurr, John Schulman, Daniel Sel-
524 sam, Kyla Sheppard, Toki Sherbakov, Jessica Shieh, Sarah Shoker, Pranav Shyam, Szymon Sidor,
525 Eric Sigler, Maddie Simens, Jordan Sitkin, Katarina Slama, Ian Sohl, Benjamin D. Sokolowsky,
526 Yang Song, Natalie Staudacher, Felipe Petroski Such, Natalie Summers, Ilya Sutskever, Jie Tang,
527 Nikolas A. Tezak, Madeleine Thompson, Phil Tillet, Amin Tootoonchian, Elizabeth Tseng, Pre-
528 ston Tuggle, Nick Turley, Jerry Tworek, Juan Felipe Cer'on Uribe, Andrea Vallone, Arun Vi-
529 jayvergyia, Chelsea Voss, Carroll L. Wainwright, Justin Jay Wang, Alvin Wang, Ben Wang,
530 Jonathan Ward, Jason Wei, CJ Weinmann, Akila Welihinda, Peter Welinder, Jiayi Weng, Lilian
531 Weng, Matt Wiethoff, Dave Willner, Clemens Winter, Samuel Wolrich, Hannah Wong, Lauren
Workman, Sherwin Wu, Jeff Wu, Michael Wu, Kai Xiao, Tao Xu, Sarah Yoo, Kevin Yu, Qiming
Yuan, Wojciech Zaremba, Rowan Zellers, Chong Zhang, Marvin Zhang, Shengjia Zhao, Tianhao
Zheng, Juntang Zhuang, William Zhuk, and Barret Zoph. Gpt-4 technical report. 2023. URL
<https://api.semanticscholar.org/CorpusID:257532815>.

532 Akari Asai, Zeqiu Wu, Yizhong Wang, Avirup Sil, and Hannaneh Hajishirzi. Self-rag: Learning
533 to retrieve, generate, and critique through self-reflection. *ArXiv*, abs/2310.11511, 2023. URL
<https://api.semanticscholar.org/CorpusID:264288947>.

534 Ingeol Baek, Hwan Chang, Byeongjeong Kim, Jimin Lee, and Hwanhee Lee. Probing-
535 rag: Self-probing to guide language models in selective document retrieval. *arXiv preprint*
arXiv:2410.13339, 2024.

536 Shijie Chen, Bernal Jiménez Gutiérrez, and Yu Su. Attention in large language models yields effi-
537 cient zero-shot re-rankers, 2024. URL <https://arxiv.org/abs/2410.02642>.

540 Wei-Lin Chiang, Zhuohan Li, Zi Lin, Ying Sheng, Zhanghao Wu, Hao Zhang, Lianmin Zheng,
 541 Siyuan Zhuang, Yonghao Zhuang, Joseph E. Gonzalez, Ion Stoica, and Eric P. Xing. Vicuna: An
 542 open-source chatbot impressing gpt-4 with 90%* chatgpt quality, March 2023. URL <https://lmsys.org/blog/2023-03-30-vicuna/>.

543

544 Florin Cuconasu, Giovanni Trappolini, Federico Siciliano, Simone Filice, Cesare Campagnano,
 545 Yoelle Maarek, Nicola Tonellootto, and Fabrizio Silvestri. The power of noise: Redefining re-
 546 trieval for RAG systems. In Grace Hui Yang, Hongning Wang, Sam Han, Claudia Hauff,
 547 Guido Zuccon, and Yi Zhang (eds.), *Proceedings of the 47th International ACM SIGIR Con-
 548 ference on Research and Development in Information Retrieval, SIGIR 2024, Washington DC,
 549 USA, July 14-18, 2024*, pp. 719–729. ACM, 2024. doi: 10.1145/3626772.3657834. URL
 550 <https://doi.org/10.1145/3626772.3657834>.

551

552 DeepSeek-AI. Deepseek-r1: Incentivizing reasoning capability in llms via reinforcement learning,
 553 2025. URL <https://arxiv.org/abs/2501.12948>.

554

555 Abhimanyu Dubey, Abhinav Jauhri, Abhinav Pandey, Abhishek Kadian, Ahmad Al-Dahle, Aiesha
 556 Letman, Akhil Mathur, Alan Schelten, Amy Yang, Angela Fan, Anirudh Goyal, Anthony
 557 Hartshorn, Aobo Yang, Archi Mitra, Archie Sravankumar, Artem Korenev, Arthur Hinsvark,
 558 Arun Rao, Aston Zhang, Aurélien Rodriguez, Austen Gregerson, Ava Spataru, Baptiste Rozière,
 559 Bethany Biron, Binh Tang, Bobbie Chern, Charlotte Caucheteux, Chaya Nayak, Chloe Bi, Chris
 560 Marra, Chris McConnell, Christian Keller, Christophe Touret, Chunyang Wu, Corinne Wong,
 561 Cristian Canton Ferrer, Cyrus Nikolaidis, Damien Allonsius, Daniel Song, Danielle Pintz, Danny
 562 Livshits, David Esiobu, Dhruv Choudhary, Dhruv Mahajan, Diego Garcia-Olano, Diego Perino,
 563 Dieuwke Hupkes, Egor Lakomkin, Ehab AlBadawy, Elina Lobanova, Emily Dinan, Eric Michael
 564 Smith, Filip Radenovic, Frank Zhang, Gabriel Synnaeve, Gabrielle Lee, Georgia Lewis Ander-
 565 son, Graeme Nail, Grégoire Mialon, Guan Pang, Guillem Cucurell, Hailey Nguyen, Hannah Ko-
 566 revaar, Hu Xu, Hugo Touvron, Iliyan Zarov, Imanol Arrieta Ibarra, Isabel M. Kloumann, Ishan
 567 Misra, Ivan Evtimov, Jade Copet, Jaewon Lee, Jan Geffert, Jana Vranes, Jason Park, Jay Ma-
 568 hadeokar, Jeet Shah, Jelmer van der Linde, Jennifer Billock, Jenny Hong, Jenya Lee, Jeremy
 569 Fu, Jianfeng Chi, Jianyu Huang, Jiawen Liu, Jie Wang, Jiecao Yu, Joanna Bitton, Joe Spisak,
 570 Jongsoo Park, Joseph Rocca, Joshua Johnstun, Joshua Saxe, Junteng Jia, Kalyan Vasuden Al-
 571 wala, Kartikeya Upasani, Kate Plawiak, Ke Li, Kenneth Heafield, Kevin Stone, and et al. The
 572 llama 3 herd of models. *CoRR*, abs/2407.21783, 2024. doi: 10.48550/ARXIV.2407.21783. URL
 573 <https://doi.org/10.48550/arXiv.2407.21783>.

574

575 Yunfan Gao, Yun Xiong, Xinyu Gao, Kangxiang Jia, Jinliu Pan, Yuxi Bi, Yi Dai, Jiawei Sun, Qianyu
 576 Guo, Meng Wang, and Haofen Wang. Retrieval-augmented generation for large language models:
 577 A survey. *ArXiv*, abs/2312.10997, 2023. URL <https://api.semanticscholar.org/CorpusID:266359151>.

578

579 Xanh Ho, Anh-Khoa Duong Nguyen, Saku Sugawara, and Akiko Aizawa. Constructing A multi-
 580 hop QA dataset for comprehensive evaluation of reasoning steps. In Donia Scott, Núria Bel,
 581 and Chengqing Zong (eds.), *Proceedings of the 28th International Conference on Compu-
 582 tational Linguistics, COLING 2020, Barcelona, Spain (Online), December 8-13, 2020*, pp. 6609–
 583 6625. International Committee on Computational Linguistics, 2020. doi: 10.18653/V1/2020.
 584 COLING-MAIN.580. URL <https://doi.org/10.18653/v1/2020.coling-main.580>.

585

586 Zixuan Ke, Weize Kong, Cheng Li, Mingyang Zhang, Qiaozhu Mei, and Michael Bendersky. Bridg-
 587 ing the preference gap between retrievers and LLMs. In Lun-Wei Ku, Andre Martins, and
 588 Vivek Srikumar (eds.), *Proceedings of the 62nd Annual Meeting of the Association for Com-
 589 putational Linguistics (Volume 1: Long Papers)*, pp. 10438–10451, Bangkok, Thailand, August
 590 2024. Association for Computational Linguistics. doi: 10.18653/v1/2024.acl-long.562. URL
 591 [https://aclanthology.org/2024.acl-long.562/](https://aclanthology.org/2024.acl-long.562).

592

593 Kiseung Kim and Jay-Yoon Lee. RE-RAG: improving open-domain QA performance and inter-
 594 pretability with relevance estimator in retrieval-augmented generation. In Yaser Al-Onaizan,
 595 Mohit Bansal, and Yun-Nung Chen (eds.), *Proceedings of the 2024 Conference on Empiri-
 596 cal Methods in Natural Language Processing, EMNLP 2024, Miami, FL, USA, November 12-
 597 16, 2024*, pp. 22149–22161. Association for Computational Linguistics, 2024. URL <https://aclanthology.org/2024.emnlp-main.1236>.

594 Sha Li and Naren Ramakrishnan. Oreo: A plug-in context reconstructor to enhance retrieval-
 595 augmented generation. *CoRR*, abs/2502.13019, 2025. doi: 10.48550/ARXIV.2502.13019. URL
 596 <https://doi.org/10.48550/arXiv.2502.13019>.
 597

598 Nelson F. Liu, Kevin Lin, John Hewitt, Ashwin Paranjape, Michele Bevilacqua, Fabio Petroni, and
 599 Percy Liang. Lost in the middle: How language models use long contexts. *Trans. Assoc. Comput.
 600 Linguistics*, 12:157–173, 2024. doi: 10.1162/TACL_A_00638. URL https://doi.org/10.1162/tacl_a_00638.
 601

602 Zhining Liu, Rana Ali Amjad, Ravinarayana Adkathimar, Tianxin Wei, and Hanghang Tong. Self-e-
 603 licit: Your language model secretly knows where is the relevant evidence. *CoRR*, abs/2502.08767,
 604 2025. doi: 10.48550/ARXIV.2502.08767. URL <https://doi.org/10.48550/arXiv.2502.08767>.
 605

606 Wen Luo, Tianshu Shen, Wei Li, Guangyue Peng, Richeng Xuan, Houfeng Wang, and Xi Yang.
 607 Halludial: A large-scale benchmark for automatic dialogue-level hallucination evaluation. *CoRR*,
 608 abs/2406.07070, 2024. doi: 10.48550/ARXIV.2406.07070. URL <https://doi.org/10.48550/arXiv.2406.07070>.
 609

610 Wen Luo, Feifan Song, Wei Li, Guangyue Peng, Shaohang Wei, and Houfeng Wang. Odysseus
 611 navigates the sirens’ song: Dynamic focus decoding for factual and diverse open-ended text
 612 generation. *CoRR*, abs/2503.08057, 2025. doi: 10.48550/ARXIV.2503.08057. URL <https://doi.org/10.48550/arXiv.2503.08057>.
 613

614 Tong Niu, Shafiq Joty, Ye Liu, Caiming Xiong, Yingbo Zhou, and Semih Yavuz. Judgerank: Lever-
 615 aging large language models for reasoning-intensive reranking. *CoRR*, abs/2411.00142, 2024.
 616 doi: 10.48550/ARXIV.2411.00142. URL <https://doi.org/10.48550/arXiv.2411.00142>.
 617

618 Ruotong Pan, Boxi Cao, Hongyu Lin, Xianpei Han, Jia Zheng, Sirui Wang, Xunliang Cai, and
 619 Le Sun. Not all contexts are equal: Teaching LLMs credibility-aware generation. In Yaser
 620 Al-Onaizan, Mohit Bansal, and Yun-Nung Chen (eds.), *Proceedings of the 2024 Conference on
 621 Empirical Methods in Natural Language Processing*, pp. 19844–19863, Miami, Florida, USA,
 622 November 2024. Association for Computational Linguistics. doi: 10.18653/v1/2024.emnlp-main.
 623 1109. URL <https://aclanthology.org/2024.emnlp-main.1109/>.
 624

625 Alexander Peysakhovich and Adam Lerer. Attention sorting combats recency bias in long con-
 626 text language models. *CoRR*, abs/2310.01427, 2023. doi: 10.48550/ARXIV.2310.01427. URL
 627 <https://doi.org/10.48550/arXiv.2310.01427>.
 628

629 Jirui Qi, Gabriele Sarti, Raquel Fernández, and Arianna Bisazza. Model internals-based answer
 630 attribution for trustworthy retrieval-augmented generation. In Yaser Al-Onaizan, Mohit Bansal,
 631 and Yun-Nung Chen (eds.), *Proceedings of the 2024 Conference on Empirical Methods in Nat-
 632 ural Language Processing, EMNLP 2024, Miami, FL, USA, November 12-16, 2024*, pp. 6037–
 633 6053. Association for Computational Linguistics, 2024. URL <https://aclanthology.org/2024.emnlp-main.347>.
 634

635 Zhen Qin, Rolf Jagerman, Kai Hui, Honglei Zhuang, Junru Wu, Le Yan, Jiaming Shen, Tianqi
 636 Liu, Jialu Liu, Donald Metzler, Xuanhui Wang, and Michael Bendersky. Large language
 637 models are effective text rankers with pairwise ranking prompting. In Kevin Duh, Helena
 638 Gómez-Adorno, and Steven Bethard (eds.), *Findings of the Association for Computational Lin-
 639 guistics: NAACL 2024, Mexico City, Mexico, June 16-21, 2024*, pp. 1504–1518. Association
 640 for Computational Linguistics, 2024. doi: 10.18653/V1/2024.FINDINGS-NAACL.97. URL
 641 <https://doi.org/10.18653/v1/2024.findings-naacl.97>.
 642

643 Freda Shi, Xinyun Chen, Kanishka Misra, Nathan Scales, David Dohan, Ed Huai hsin Chi,
 644 Nathanael Scharli, and Denny Zhou. Large language models can be easily distracted by ir-
 645 relevant context. In *International Conference on Machine Learning*, 2023. URL <https://api.semanticscholar.org/CorpusID:256459776>.
 646

647 Weijia Shi, Sewon Min, Michihiro Yasunaga, Minjoon Seo, Richard James, Mike Lewis, Luke
 Zettlemoyer, and Wen-tau Yih. REPLUG: retrieval-augmented black-box language models.

648 In Kevin Duh, Helena Gómez-Adorno, and Steven Bethard (eds.), *Proceedings of the 2024*
 649 *Conference of the North American Chapter of the Association for Computational Linguistics:*
 650 *Human Language Technologies (Volume 1: Long Papers)*, NAACL 2024, Mexico City, Mex-
 651 *ico, June 16-21, 2024*, pp. 8371–8384. Association for Computational Linguistics, 2024. doi:
 652 10.18653/V1/2024.NAACL-LONG.463. URL <https://doi.org/10.18653/v1/2024.naacl-long.463>.

653

654 Weiwei Sun, Lingyong Yan, Xinyu Ma, Shuaiqiang Wang, Pengjie Ren, Zhumin Chen, Dawei Yin,
 655 and Zhaochun Ren. Is chatgpt good at search? investigating large language models as re-ranking
 656 agents. In Houda Bouamor, Juan Pino, and Kalika Bali (eds.), *Proceedings of the 2023 Con-
 657 ference on Empirical Methods in Natural Language Processing, EMNLP 2023, Singapore, De-
 658 cember 6-10, 2023*, pp. 14918–14937. Association for Computational Linguistics, 2023. doi:
 659 10.18653/V1/2023.EMNLP-MAIN.923. URL <https://doi.org/10.18653/v1/2023.emnlp-main.923>.

660

661 Hugo Touvron, Louis Martin, Kevin R. Stone, Peter Albert, Amjad Almahairi, Yasmine Babaei,
 662 Nikolay Bashlykov, Soumya Batra, Prajjwal Bhargava, Shruti Bhosale, Daniel M. Bikel, Lukas
 663 Blecher, Cristian Cantón Ferrer, Moya Chen, Guillem Cucurull, David Esiobu, Jude Fernan-
 664 des, Jeremy Fu, Wenyin Fu, Brian Fuller, Cynthia Gao, Vedanuj Goswami, Naman Goyal, An-
 665 thony S. Hartshorn, Saghar Hosseini, Rui Hou, Hakan Inan, Marcin Kardas, Viktor Kerkez, Ma-
 666 dian Khabsa, Isabel M. Kloumann, A. V. Korenev, Punit Singh Koura, Marie-Anne Lachaux,
 667 Thibaut Lavril, Jenya Lee, Diana Liskovich, Yinghai Lu, Yuning Mao, Xavier Martinet, Todor Mi-
 668 haylov, Pushkar Mishra, Igor Molybog, Yixin Nie, Andrew Poulton, Jeremy Reizenstein, Rashi
 669 Rungta, Kalyan Saladi, Alan Schelten, Ruan Silva, Eric Michael Smith, R. Subramanian, Xia
 670 Tan, Binh Tang, Ross Taylor, Adina Williams, Jian Xiang Kuan, Puxin Xu, Zhengxu Yan, Iliyan
 671 Zarov, Yuchen Zhang, Angela Fan, Melanie Kambadur, Sharan Narang, Aurelien Rodriguez,
 672 Robert Stojnic, Sergey Edunov, and Thomas Scialom. Llama 2: Open foundation and fine-tuned
 673 chat models. *ArXiv*, abs/2307.09288, 2023. URL <https://api.semanticscholar.org/CorpusID:259950998>.

674

675 Harsh Trivedi, Niranjan Balasubramanian, Tushar Khot, and Ashish Sabharwal. Musique: Multi-
 676 hop questions via single-hop question composition. *Trans. Assoc. Comput. Linguistics*, 10:539–
 677 554, 2022. doi: 10.1162/TACL_A_00475. URL https://doi.org/10.1162/tacl_a_00475.

678

679 Yiteng Tu, Weihang Su, Yujia Zhou, Yiqun Liu, and Qingyao Ai. Rbft: Robust fine-tuning for
 680 retrieval-augmented generation against retrieval defects. *CoRR*, abs/2501.18365, 2025. doi: 10.
 681 48550/ARXIV.2501.18365. URL <https://doi.org/10.48550/arXiv.2501.18365>.

682

683 Yuhao Wang, Ruiyang Ren, Junyi Li, Xin Zhao, Jing Liu, and Ji-Rong Wen. REAR: A relevance-
 684 aware retrieval-augmented framework for open-domain question answering. In Yaser Al-Onaizan,
 685 Mohit Bansal, and Yun-Nung Chen (eds.), *Proceedings of the 2024 Conference on Empiri-
 686 cal Methods in Natural Language Processing, EMNLP 2024, Miami, FL, USA, November 12-
 687 16, 2024*, pp. 5613–5626. Association for Computational Linguistics, 2024. URL <https://aclanthology.org/2024.emnlp-main.321>.

688

689 Siye Wu, Jian Xie, Jiangjie Chen, Tinghui Zhu, Kai Zhang, and Yanghua Xiao. How easily do
 690 irrelevant inputs skew the responses of large language models? In *First Conference on Language
 691 Modeling*, 2024. URL <https://openreview.net/forum?id=S7NVVfuRv8>.

692

693 Chong Xiang, Tong Wu, Zexuan Zhong, David A. Wagner, Danqi Chen, and Prateek Mittal. Cer-
 694 tifiably robust RAG against retrieval corruption. *CoRR*, abs/2405.15556, 2024. doi: 10.48550/
 695 ARXIV.2405.15556. URL <https://doi.org/10.48550/arXiv.2405.15556>.

696

697 Jian Xie, Kai Zhang, Jiangjie Chen, Renze Lou, and Yu Su. Adaptive chameleon or stubborn sloth:
 698 Revealing the behavior of large language models in knowledge conflicts. In *The Twelfth Inter-
 699 national Conference on Learning Representations, ICLR 2024, Vienna, Austria, May 7-11, 2024*.
 700 OpenReview.net, 2024. URL <https://openreview.net/forum?id=auKAUJZMO6>.

701

702 Peng Xu, Wei Ping, Xianchao Wu, Lawrence McAfee, Chen Zhu, Zihan Liu, Sandeep Sub-
 703 ramanian, Evelina Bakhturina, Mohammad Shoeybi, and Bryan Catanzaro. Retrieval meets
 704 long context large language models. In *The Twelfth International Conference on Learning*

702 *Representations, ICLR 2024, Vienna, Austria, May 7-11, 2024*. OpenReview.net, 2024. URL
 703 <https://openreview.net/forum?id=xw5nxFWMlo>.

704

705 Shi-Qi Yan, Jia-Chen Gu, Yun Zhu, and Zhen-Hua Ling. Corrective retrieval augmented generation.
 706 *arXiv preprint arXiv:2401.15884*, 2024.

707

708 An Yang, Baosong Yang, Beichen Zhang, Binyuan Hui, Bo Zheng, Bowen Yu, Chengyuan Li,
 709 Dayiheng Liu, Fei Huang, Haoran Wei, Huan Lin, Jian Yang, Jianhong Tu, Jianwei Zhang, Jianxin
 710 Yang, Jiaxi Yang, Jingren Zhou, Junyang Lin, Kai Dang, Keming Lu, Keqin Bao, Kexin Yang,
 711 Le Yu, Mei Li, Mingfeng Xue, Pei Zhang, Qin Zhu, Rui Men, Runji Lin, Tianhao Li, Tingyu
 712 Xia, Xingzhang Ren, Xuancheng Ren, Yang Fan, Yang Su, Yichang Zhang, Yu Wan, Yuqiong
 713 Liu, Zeyu Cui, Zhenru Zhang, and Zihan Qiu. Qwen2.5 technical report. *CoRR*, abs/2412.15115,
 714 2024. doi: 10.48550/ARXIV.2412.15115. URL <https://doi.org/10.48550/arXiv.2412.15115>.

715

716 ZhiLin Yang, Peng Qi, Saizheng Zhang, Yoshua Bengio, William W. Cohen, Ruslan Salakhutdinov,
 717 and Christopher D. Manning. Hotpotqa: A dataset for diverse, explainable multi-hop question
 718 answering. In Ellen Riloff, David Chiang, Julia Hockenmaier, and Jun’ichi Tsujii (eds.), *Pro-
 719 ceedings of the 2018 Conference on Empirical Methods in Natural Language Processing, Brus-
 720 sels, Belgium, October 31 - November 4, 2018*, pp. 2369–2380. Association for Computational
 721 Linguistics, 2018. doi: 10.18653/V1/D18-1259. URL <https://doi.org/10.18653/v1-d18-1259>.

722

723 Ori Yoran, Tomer Wolfson, Ori Ram, and Jonathan Berant. Making retrieval-augmented language
 724 models robust to irrelevant context. In *The Twelfth International Conference on Learning Repre-
 725 sentations*, 2024. URL <https://openreview.net/forum?id=ZS4m74kZpH>.

726

727 Huichi Zhou, Kin-Hei Lee, Zhonghao Zhan, Yue Chen, Zhenhao Li, Zhaoyang Wang, Hamed Had-
 728 dadi, and Emine Yilmaz. Trustrag: Enhancing robustness and trustworthiness in RAG. *CoRR*,
 729 abs/2501.00879, 2025. doi: 10.48550/ARXIV.2501.00879. URL <https://doi.org/10.48550/arXiv.2501.00879>.

730

731

732

733

734 **A LLM USAGE**

735

736 Large Language Models (LLMs) are increasingly utilized in scientific research and provide substan-
 737 tial support in academic writing. Their applications range from enhancing grammar and wording to
 738 assisting in the drafting of complete manuscript sections. In this paper, we employed an LLM solely
 739 for language refinement aimed at improving clarity and explanatory quality. All content has been
 740 thoroughly verified for factual accuracy, and the authors take full responsibility for the entirety of
 741 the work. The central ideas, experimental design, and methodological framework were developed
 742 independently by the authors without the use of LLMs.

743

744 **B DETAILS ABOUT PRELIMINARY EXPERIMENTS**

745

746 **B.1 DATASETS**

747

748 We applied the datasets processed by Pan et al. (2024) in our paper. Due to resource limitations, we
 749 mainly focus on several open-domain variants of the datasets.

750

751 HotpotQA (Yang et al., 2018) and 2WikiMHQA (Ho et al., 2020) both require reasoning across
 752 multiple documents, and feature a high proportion of distracting documents. Importantly, the data
 753 from HotpotQA is extracted from the dev subset, whereas our training dataset is derived from the
 754 train subset. Musique (Trivedi et al., 2022) questions are of higher complexity, with up to 90% of
 755 distracting passages.

See original paper (Pan et al., 2024) for more details.

756 B.2 IMPLEMENTATION DETAILS
757

758 We will list the details of hyperparameters we used in the experiments. The seed is set to 42. The
759 temperate is set to 0.01 and the number of max_new_tokens is 300. The same prompt template is
760 used for all datasets and all models in the experiments to exclude template interference, which is
761 presented as follows:

762
763
764 You’re a helpful AI assistant. The assistant answers questions based on given passages.
765
766 Docs: $\{\{d_0.\text{title}\}\}:\{\{d_0.\text{text}\}\}$
767 $\{\{d_1.\text{title}\}\}:\{\{d_1.\text{text}\}\}$
768 $\{\{d_2.\text{title}\}\}:\{\{d_2.\text{text}\}\}$
769
770 (more passages) ...
771
772 Question: $\{\{\text{question}\}\}$
773
774 Answer:
775
776

777 C MIRAGE RESULTS
778

779 An ordered placement approach such as placing
780 relevant documents close to the questions is
781 a powerful baseline, but we want to make bet-
782 ter use of the model’s positional bias. There-
783 fore, we first explore the dependency of the
784 generated answer token on the context doc-
785 ments using the library developed by Qi et al.
786 (2024). MIRAGE identifies context-sensitive
787 answer tokens and aligns them with retrieved
788 documents based on internal model states. We
789 further analyze the positional distribution of
790 context documents that answer tokens attend to
791 most.

792 The results of vicuna-7b, llama3-8b, qwen-7b,
793 and qwen-7b-instruct are presented in Figure
794 5a, 5b, 5c, and 5d, respectively.

795 The different rows represent the results on different datasets: HotpotQA, Musique, 2wikiMulti-
796 HopQA. The different columns represent the different ways of composing the prompt: unorder-
797 ed (concat) or ordered (rerank). In each figure, the horizontal axis represents document positions within
798 the prompt, ranging from position 0 (beginning) to position $N - 1$ (end, closest to the question). The
799 vertical bar indicates the number of answer tokens that depend on the document located at each
800 corresponding position.

801 The results show that under ordered input, it is common sense to depend on the documents near the
802 question. In contrast, it shows a clear positional bias towards the beginning and the end under un-
803 ordered input, which matches the Lost-in-the-middle (Liu et al., 2024) phenomenon in performance.
804 And this is more evident on the Musique which has a larger number of documents.

805
806 D ATTENTION WEIGHT RESULTS
807

808 The complete Attention Weight Results are presented here.
809

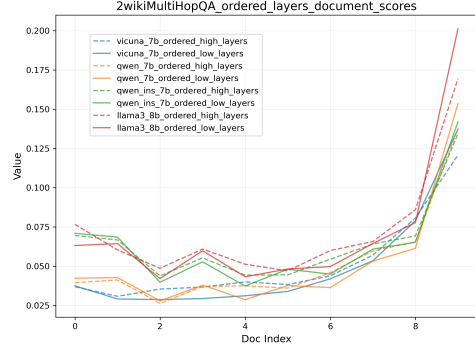
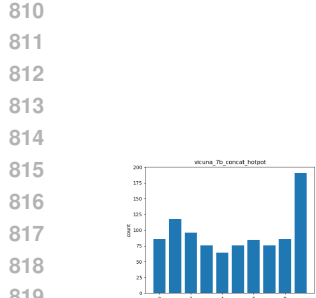
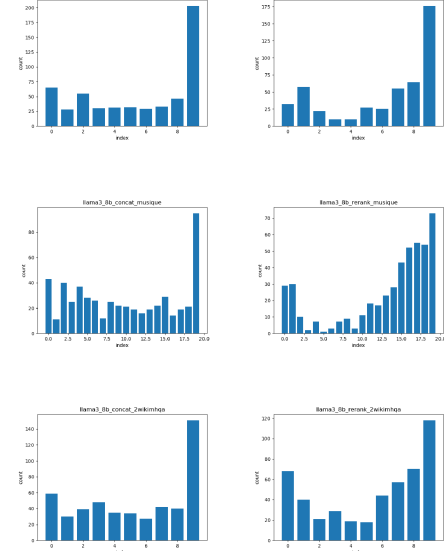


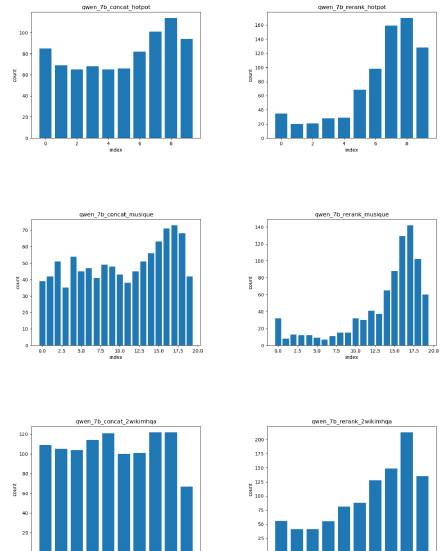
Figure 4: The document scores S of all models with different selected layers on 2wikiMulti-HopQA datasets under ordered input.



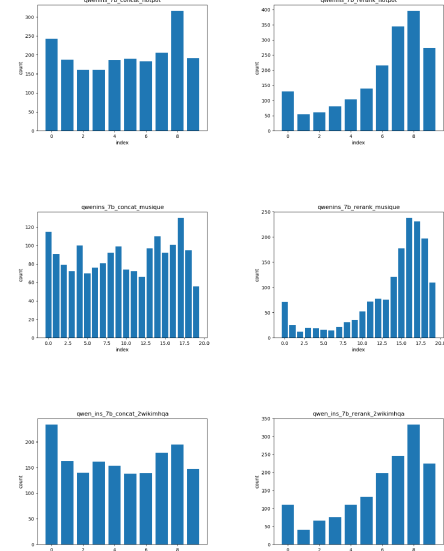
(a) The MIRAGE results of vicuna-7b model.



(b) The MIRAGE results of llama3-8b model.



(c) The MIRAGE results of qwen-7b model.



(d) The MIRAGE results of qwen-7b-instruct model.

858
859
860
861
862
863

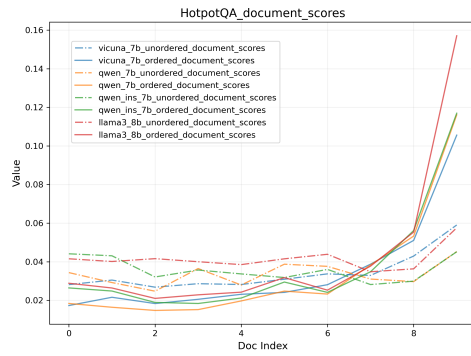
Figure 5: The MIRAGE results of all models. For each model, the different lines represent different datasets: HotpotQA, Musique, 2wikiMultiHopQA. The first and second columns represent the un-ordered and ordered inputs.

864
865

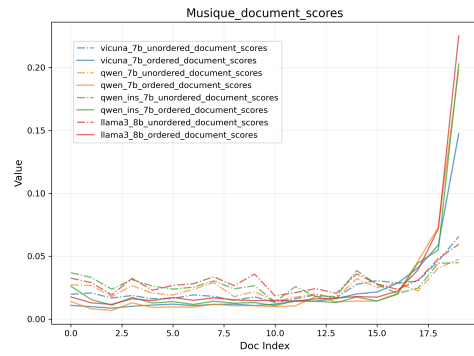
D.1 HORIZONTAL RESULTS

866
867
868
869
870

We present the complete results of the difference between the score of different documents in different order of documents in this section. The results on HotpotQA dataset is presented in Figure 6a, and the results on Musique dataset is presented in Figure 6b.

871
872
873
874
875
876
877
878
879
880
881

(a) The document scores S of all models on HotpotQA datasets.



(b) The document scores S of all models on Musique datasets.

882
883
884
885
886
887

Figure 6: The document scores S of all models on HotpotQA datasets. The solid line - corresponds to the ordered input, the dashed - line corresponds to the unordered input, and the results of the same model are shown in the same color.

888
889
890
891

D.2 VERTICAL RESULTS

892
893
894

We present the complete results of different selected layers in this section. See Figure 4,7a, 7b,7c,7d for more information.

895
896
897

D.3 POSITIONAL SCORES

898
899
900
901

We present the complete results of postional scores on all datasets in this section. See Figure 8a,8b for more information.

902
903
904
905
906
907
908
909
910
911
912

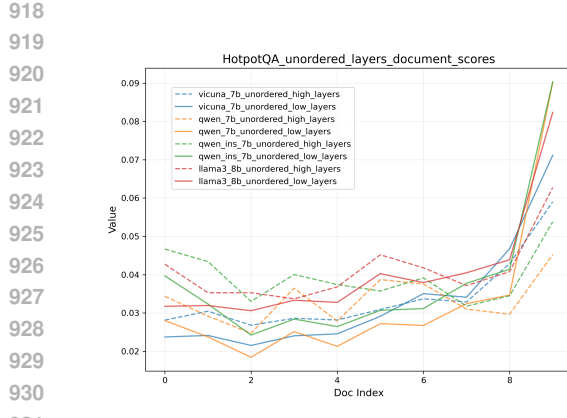
E EXAMPLES OF DIFFERENT ORDERING

The goal of original ranking and U-shaped Placement is to place good documents in good positions, but the default good positions are different. As an example, if the dataset has 10 documents, the order of documents under the ordered input is $[0,1,\dots,9]$, the question is placed at the end, document 9 has the best relevance, and document 0 has the worst relevance. After placing the documents according to the positional bias under the U-shaped Placement, the order of documents may become $[6,5,4,2,0,1,3,7,8,9]$, and the question is placed at the end as well. While the reverse version of ordered has the input document order as $[9,8,\dots,0]$, and the reverse version of U-shaped Placement has the document order $[3,4,5,7,9,8,6,2,1,0]$, with bad documents prioritized to occupy the default good placements in each reverse order.

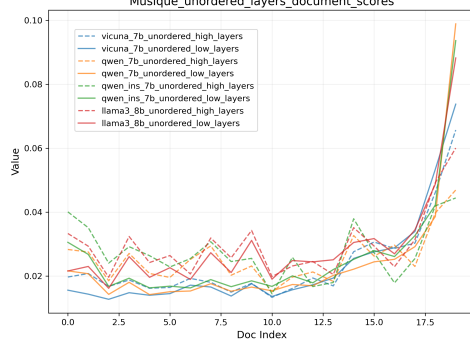
913
914
915
916
917

F RANKGPT

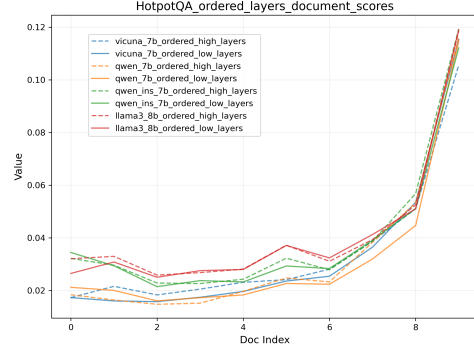
The prompt template used during the first round of RankGPT generation is as follows, based on which the prompts are constructed to allow LLM to perform listwise document sorting.



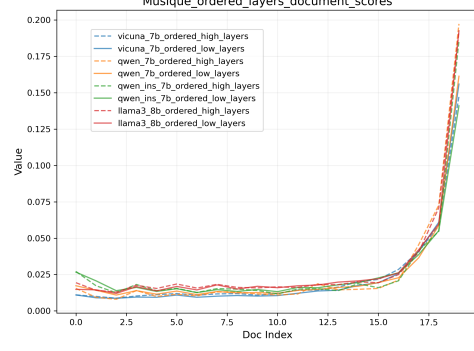
931 (a) The document scores S of all models with
932 different selected layers on Hotpot datasets under
933 unordered input.



945 (c) The document scores S of all models with
946 different selected layers on Musique datasets under
947 unordered input.

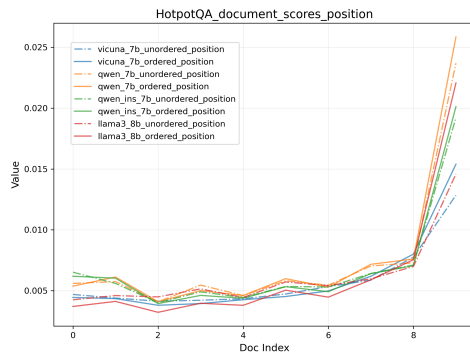


948 (b) The document scores S of all models with
949 different selected layers on Hotpot datasets under
950 ordered input.

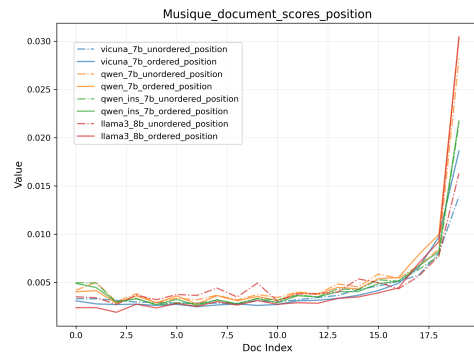


954 (d) The document scores S of all models with
955 different selected layers on Musique datasets under
956 ordered input.

957 Figure 7: The document scores S of all models with different selected layers. The solid - and dotted - lines are used to distinguish the first and the last half of layers. And the results of the same model are shown in the same color.



966 (a) The positional scores S of all models on HotpotQA datasets.



966 (b) The positional scores S of all models on Musique datasets.

967 Figure 8: The positional scores S of all models, which are calculated by aggregating the document
968 scores of the previous token and the terminating token of the answer tokens.

972
973
974
975 Table 6: Results of the different document relevance sorting methods of vicuna-7b model under
976 ordered input. Calibration means subtracting positional influence from attention scores.
977
978
979

Ranking	Aggregation	H	M	W
Retrieval	-	0.4	0.312	0.482
Attention Weight	answer calibration	0.406 0.398	0.305 0.279	0.494 0.496

980
981
982 This is RankGPT, an intelligent assistant that can rank passages based on their relevancy to
983 the query.
984

985 The following are $\{\{\text{num}\}\}$ passages, each indicated by number identifier $[\cdot]$. I can rank
986 them based on their relevance to query: $\{\{\text{query}\}\}$
987

988 [1] $\{\{\text{passage_1}\}\}$
989

990 [2] $\{\{\text{passage_2}\}\}$
991

992 (more passages) ...
993

994 The search query is: $\{\{\text{query}\}\}$
995

996 I will rank the $\{\{\text{num}\}\}$ passages above based on their relevance to the search query. The
997 passages will be listed in descending order using identifiers, and the most relevant passages
998 should be listed first, and the output format should be $[\cdot] \downarrow [\cdot] \downarrow \dots$ etc, e.g., [1] \downarrow [2] \downarrow etc.
999

1000 The ranking results of the $\{\{\text{num}\}\}$ passages (only identifiers) is:
1001
1002

1003 G SOMETHING WE TRIED

1004
1005 The complete pipeline of our proposed algorithm is embodied in Algorithm 2, while in this section
1006 we briefly describe some additional attempts at details.
1007

1008 First, we address the estimation of document relevance. In previous experiments, we directly utilized
1009 document scores as the basis for estimation. The calibration method introduced by Chen et al.
1010 (2024) offers a valuable inspiration. Accordingly, we also attempt to remove positional effects from
1011 the attention scores. Specifically, we subtract the positional scores from the document relevance
1012 scores. However, this approach yields no significant improvement, likely because the answer-based
1013 aggregation scores and the positional representations (derived from start and end tokens) are not
1014 strictly commensurable. The corresponding results are provided in G.1.

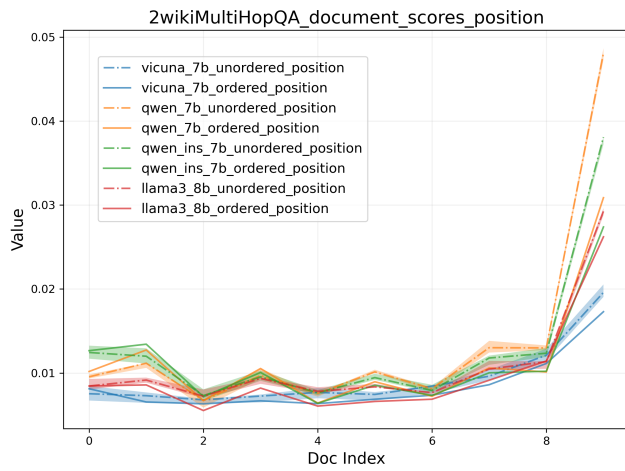
1015 We place the documents according to the U-shape in our proposed method, however, the positional
1016 bias does not exactly fit the U-shape and there may be zigzag in the middle, as shown in previous
1017 analysis. Aggregating the token-level position scores by document and then placing the document
1018 directly according to the result of document-level has no zigzag problem, but it has length problem
1019 as said in section 4. Is the length issue more important or the zigzag issue? The results in G.2
1020 show that placement according to the U-shape is more in line with the positional bias, and the length
1021 mismatch has a greater impact on performance compared to the zigzag problem.
1022

1023 G.1 CALIBRATION

1024 As in section 6.2, the vicuna model was also used in the experiments under the ordered input and
1025 the results are presented in Table 6.

1026
 1027 Table 7: Results of different placements after sorting them for relevance based on external search
 1028 scores. Default means directly placing the relevant ones close to the questions, while U-shaped
 1029 is our proposed method in accordance with positional bias. Direct-U means aggregating token-
 1030 level position scores by document and then placing the document directly according to the result of
 1031 document-level.

Placement	Vicuna-7b			Llama-3.1-8b			Qwen2.5-7b			Qwen2.5-7b-ins		
	H	M	W	H	M	W	H	M	W	H	M	W
Default	0.4	0.312	0.482	0.302	0.238	0.358	0.408	0.342	0.41	0.472	0.5	0.526
U-shaped (Our)	0.397	0.314	0.524	0.31	0.252	0.376	0.416	0.369	0.414	0.486	0.509	0.522
Direct-U	0.39	0.291	0.49	0.31	0.232	0.356	0.406	0.361	0.406	0.472	0.495	0.516



1053 Figure 9: The results from five repeated experiments. The shaded area indicates the range of score
 1054 variations across these five random experiments.

G.2 ZIGZAG

1055
 1056 The results are presented in Table 7.

H RANDOM VARIATION

1063 To eliminate the impact of random variation while enhancing the credibility of our conclusions, we
 1064 conduct repeated experiments using different random number seeds for experiments in Figure 3. We
 1065 plotted the range of variation in the results from five repeated experiments as shaded areas in the
 1066 figure 9 .

1067 The results demonstrate that even with multiple randomizations of document order, the calculated
 1068 outcomes exhibit a certain degree of stability.

1069
 1070
 1071
 1072
 1073
 1074
 1075
 1076
 1077
 1078
 1079